Saudi Journal of Biological Sciences 28 (2021) 4421–4429

Contents lists available at ScienceDirect

Saudi Journal of Biological Sciences

journal homepage: www.sciencedirect.com

Original article

Whole exome sequencing, in silico and functional studies confirm the association of the *GJB2* mutation p.Cys169Tyr with deafness and suggest a role for the *TMEM59* gene in the hearing process

Mona Mahfood [a], Jihen Chouchen [b], Walaa Kamal Eddine Ahmad Mohamed [b], Abdullah Al Mutery [a,b], Rania Harati [c], Abdelaziz Tlili [a,b,*]

[a] Department of Applied Biology, College of Sciences, University of Sharjah, Sharjah, United Arab Emirates
[b] Human Genetics and Stem Cell Research Group, Research Institute of Sciences and Engineering, University of Sharjah, Sharjah, United Arab Emirates
[c] Department of Pharmacy Practice and Pharmacotherapeutics, College of Pharmacy, University of Sharjah, Sharjah, United Arab Emirates

ARTICLE INFO

Article history:
Received 6 December 2020
Revised 11 April 2021
Accepted 12 April 2021
Available online 20 April 2021

Keywords:
Whole exome sequencing
GJB2 gene
Missense mutation
Non-syndromic hearing loss

ABSTRACT

The development of next generation sequencing techniques has facilitated the detection of mutations at an unprecedented rate. These efficient tools have been particularly beneficial for extremely heterogeneous disorders such as autosomal recessive non-syndromic hearing loss, the most common form of genetic deafness. *GJB2* mutations are the most common cause of hereditary hearing loss. Amongst them the NM_004004.5: c.506G > A (p.Cys169Tyr) mutation has been associated with varying severity of hearing loss with unclear segregation patterns. In this study, we report a large consanguineous Emirati family with severe to profound hearing loss fully segregating the *GJB2* missense mutation p.Cys169Tyr. Whole exome sequencing (WES), in silico, splicing and expression analyses ruled out the implication of any other variants and confirmed the implication of the p.Cys169Tyr mutation in this deafness family. We also show preliminary murine expression analysis that suggests a link between the *TMEM59* gene and the hearing process. The present study improves our understanding of the molecular pathogenesis of hearing loss. It also emphasizes the significance of combining next generation sequencing approaches and segregation analyses especially in the diagnosis of disorders characterized by complex genetic heterogeneity.

Abbreviations: WES, Whole exome sequencing; HL, Hearing loss; NSHL, Non-syndromic hearing loss; NGS, next generation sequencing; GJB2, *Gap Junction Protein Beta 2*; Cx26, Connexin 26; ARNSHL, autosomal recessive non-syndromic hearing loss; UAE, United Arab Emirates; BWA, Burrows-Wheeler Aligner; SAM, Sequence Alignment/Map; BAM, Binary Alignment Map; dpSNP, Single Nucleotide Polymorphism Database; gnomAD, genome aggregation database; PolyPhen-2, Polymorphism Phenotyping v2; SIFT, Sorting Intolerant From Tolerant; PROVEAN, Protein Variation Effect Analyzer; *TMEM59*, *Transmembrane Protein 59*; SJL, Swiss Jim Lambert; *Actb*, *Actin beta*; gEAR, gene Expression Analysis Resource; *HHLA1*, *HERV-H LTR-Associating 1*; *KCNQ3*, *Potassium Voltage-Gated Channel Subfamily Q Member 3*; *ST3GAL1*, *ST3 Beta-Galactoside Alpha-2,3-Sialyltransferase 1*; *ESRRAP2*, *Estrogen-Related Receptor Alpha Pseudogene 2*; *SPATA13*, *Spermatogenesis Associated 13*; *C1QTNF9*, *C1q and TNF related 9*; VariMAT, Variation and Mutation Annotation Toolkit; RFLP, restriction fragment length polymorphism; RT-PCR, reverse transcription PCR; RT-qPCR, quantitative reverse transcription PCR; qPCR, quantitative PCR; ROH, runs of homozygosity.

* Corresponding author at: Department of Applied Biology, College of Sciences, University of Sharjah, Building W8 - Room 107, Sharjah, P.O. Box: 27272, United Arab Emirates.

E-mail address: atlili@sharjah.ac.ae (A. Tlili).

Peer review under responsibility of King Saud University.

Production and hosting by Elsevier

https://doi.org/10.1016/j.sjbs.2021.04.036
1319-562X/

1. Introduction

Hearing loss (HL) is the most common sensory deficit with an incidence of 1–3 cases in every 1,000 births (Morton and Nance, 2006). Hereditary cases account for more than 50% of HL prelingual cases (Marazita et al., 1993) meanwhile environmental and age related HL account for the remaining percentage (Bouzid et al., 2018a; Bouzid et al., 2018b). Non-syndromic hearing loss (NSHL) is the most frequent form of genetic deafness and predominately follows an autosomal recessive mode of inheritance. To date, 123 genes and over 160 loci have been linked to NSHL (https://hereditaryhearingloss.org/). The genetic heterogeneity of NSHL often impedes its diagnosis, reinforcing the utmost urgency for developing efficient and affordable diagnostic techniques.

Although traditional approaches have led to great insights into the underlying genetic causes of NSHL, the advent of next generation sequencing (NGS) has expedited the discovery of novel NSHL genes and mutations (Souissi et al., 2021). In fact, NGS-based platforms have been involved in the identification of more than 40% of NSHL genes known today (https://hereditaryhearingloss.org/). Given the time and cost effectiveness of NGS, it is expected to reveal many more NSHL genes and ultimately assist in unraveling the molecular etiology of HL (Vona et al., 2015).

Connexins are a family of transmembrane proteins that form channels known as gap junctions. These channels facilitate direct intercellular communication which is vital for the development, function, and homeostasis of various tissues and organs. Around twenty different human connexin genes have been reported (Sohl and Willecke, 2004), among them the *Gap Junction Beta 2* (*GJB2*) gene which encodes connexin 26 (Cx26) is considered the most prevalent gene causing deafness in most populations (Chan and Chang, 2014; Kelsell et al., 1997) with over 200 pathogenic variants identified so far (http://deafnessvariationdatabase.org/). The Cx26 mutation p.Cys169Tyr was first reported as being pathogenic in 2014 where it showed partial segregation in a consanguineous middle-eastern family (Birkenhager et al., 2014). This partial segregation associated with p.Cys169Tyr was observed along with HL of varying severity in another study shortly after (Zonta et al., 2015). Although many bioinformatic tools and databases such as ClinVar (https://www.ncbi.nlm.nih.gov/clinvar/) and Deafness Variation Database (https://deafnessvariationdatabase.org/) classify this variant as pathogenic, evidence associating this variant with full segregation is extremely sparse.

In the present study, WES, Sanger sequencing, in silico, splicing and expression analyses were carried out for a consanguineous Emirati family with autosomal recessive non-syndromic hearing loss (ARNSHL). Our results demonstrated that the missense variant NM_004004.5:c.506G > A (p.Cys169Tyr) is the causative mutation in the investigated family. To the best of our knowledge this is the first study to report the p.Cys169Tyr mutation with full segregation with the HL phenotype.

2. Materials and methods

2.1. Subjects and clinical assessment

A consanguineous Emirati family affected with NSHL was recruited from the UAE Deaf Association for the purpose of this study (Fig. 1). To rule out the involvement of environmental factors in the manifestation of deafness, affected family members were evaluated based on clinical history as well as physical and audiological examination including pure tone audiometry test for air and bone conduction. A summary of our strategy used to identify the responsible mutation is given as a flowchart (Fig. 2). Additionally, 107 HL patients and 50 deafness free controls from the United Arab Emirates (UAE) participated in this study. Saliva samples were collected from all subjects and genomic DNA was then extracted from these samples using the Oragene-DNA Kit (OG-500, DNA Genotek, Canada) according to manufacturer's protocol. Extracted DNA was quantified by the NanoDrop One Microvolume UV–Vis Spectrophotometer (Themo Fisher Scientific, USA). To protect the anonymity of participants, only codes were used to label all DNA samples. Written informed consents were obtained from all subjects or their parents (for participants under the age of 18) attesting their willingness to participate in this study. Moreover, all experimental procedures and informed consents used in this study were approved by the University of Sharjah Research Ethics Committee (No. REC-15-11-P004) and performed in accordance with the relevant guidelines and regulations.

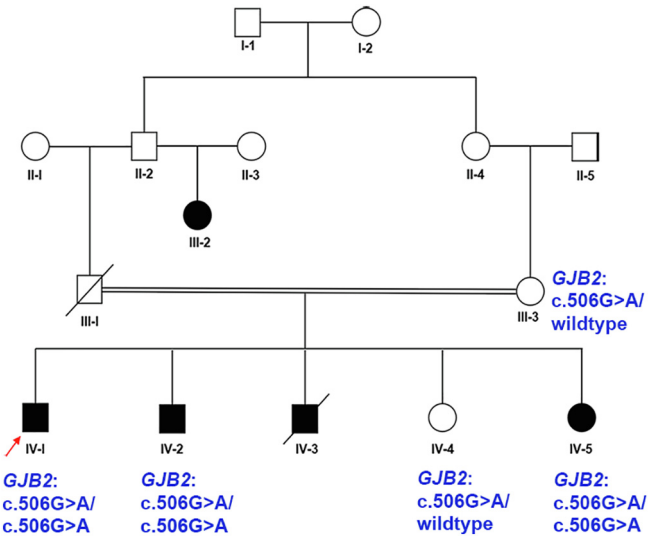

Fig. 1. Pedigree of the Emirati NSHL family. Genotypes (blue) correspond to the *GJB2* pathogenic variant NM_004004.5: c.506G > A (p.Cys169Tyr). Arrow denotes the proband.

2.2. Whole exome sequencing and in silico analysis

Whole exome sequencing followed by standard data analysis was performed using genomic DNA of individuals III-3, IV-1, IV-2, IV-4, and IV-5 (Fig. 1). In short, genomic DNA was sheared using Covaris S2 (Covaris, MA, USA) and SureSelect XT (Agilent Technologies, Santa Clara, CA, USA) was used to perform end-repair, A-addition and adaptor ligation reactions. Exome capture and enrichment were carried out using the SureSelect All Exon V5 kit (Agilent Technologies, Santa Clara, CA, USA) according to manufacturers' protocol. Post-enrichment libraries were pooled, and sequencing was then carried out using the Illumina HiSeq 2500 System (Illumina, San Diego, CA, USA). Next, paired end (2 × 100 bases) reads that passed the quality control (i.e Phred score > 20) underwent adaptor trimming and end repair using Fastq-mcf (ea-utils-1.1.2-806) and were mapped to the human reference genome build hg19/GRCh37 using Burrows-Wheeler Aligner (BWA) (Li and Durbin, 2010). Sequence Alignment/Map (SAM) tools (Li, H. et al., 2009) was then used for processing Binary Alignment Map (BAM) files. Variants from processed BAM files were then called by Genome Analysis Tool Kit (GATK) v2.7.2 (McKenna et al., 2010). Next, called variants were annotated in-house by Variation and Mutation Annotation Toolkit (VariMAT) v2.3.9 and filtered by read depth (i.e ≥ 10). The remaining variants were then further filtered by frequency (i.e < 0.01%) in Single Nucleotide Polymorphism Database (dbSNP) (https://www.ncbi.nlm.nih.gov/snp/), genome aggrega-

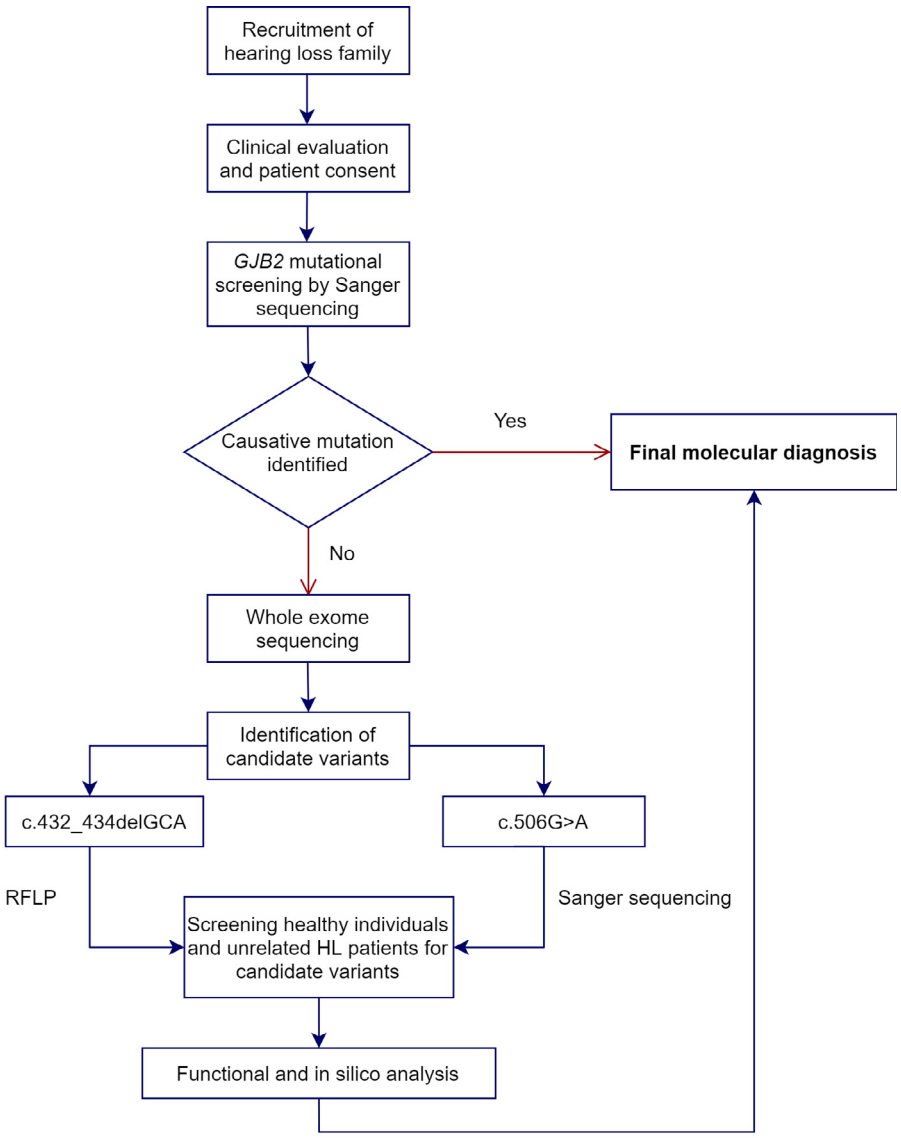

Fig. 2. Summary of the molecular diagnostic approach. The recruited HL family was first screened for *GJB2* mutations. Since the causative mutation could not be confirmed, WES was performed. After analysis, unrelated HL and healthy controls were screened for the identified candidate variants. This was followed by functional and in silico analysis of the identified candidate variants. Collectively, the outcomes of these analyses led to a final molecular diagnosis.

tion database (gnomAD) (https://gnomad.broadinstitute.org/), or Ensembl (https://www.ensembl.org/index.html).

Finally, the functional impact of the identified candidate variants was predicted using several bioinformatic tools including: Variant Effect Predictor (VEP) (http://grch37.ensembl.org/Homo_sapiens/Tools/VEP), MutationTaster (http://www.mutationtaster.org/), VarSome (https://varsome.com/), Protein Variation Effect Analyzer (PROVEAN) (http://provean.jcvi.org/index.php), Polymorphism Phenotyping v2 (PolyPhen-2) (http://genetics.bwh.harvard.edu/pph2/), Sorting Intolerant From Tolerant (SIFT) (Kumar et al., 2009) and Human Splicing Finder version 3.1 (http://www.umd.be/HSF/).

2.3. Sanger sequencing

To ensure the segregation of the identified candidate variants with the deafness phenotype, Sanger sequencing was performed using genomic DNA of individuals III-3, IV-1, IV-2, IV-4, and IV-5 (Fig. 1). In brief, PCR products corresponding to the second exon of the *GJB2* gene were generated using primers Cx26 2F and Cx26 2R, while amplicons corresponding to the third exon of the *Transmembrane Protein 59* (*TMEM59)* gene were generated using primers gDNA_TM59_3F and gDNA_TM59_3R (Table 1). PCR products were

Table 1
Primers.

Primer Name	Sequence
Cx26 2F	5′-ACACGTTCAAGAGGGTTTGG- 3′
Cx26 2R	5′-GGGAAATGCTAGCGACTGAG- 3′
gDNA_TM59_3F	5′-CCAAATTTGGAAATTCACATTGATG- 3′
gDNA_TM59_3R	5′-GGATCAAGTGGGTGATAAACACTTC- 3′
TM59 _3F_BstelI	5′-AAGGTAACCCCAAATTTGGAAATTCACATTGATG-3′
TM59_3R_NheI	5′-AAGCTAGCGGATCAAGTGGGTGATAAACACTTC-3′
EX13	5′-GGAAGACGAGCCACCTGAGC-3′
T7	5′TAATACGACTCACTATAGGG-3′
Sp6	5′-ATTTAGGTGACACTATAG-3′
cDNA_Mouse_1F	5′-TACCCCTTGCACACCTACCCGAAG-3′
cDNA_Mouse_4R	5′-CATTCTTGGCATCAGGGACATGAG-3′
Mouse Actb F	5′- AGCTTCTTTGCAGCTCCTTC–3′
Mouse Actb R	5′- CCACCATCACACCCTGGT –3′

then treated with ExoSAP-IT PCR Product Cleanup Reagent (78200.200.UL, Applied Biosystems, Thermo Fisher Scientific, USA) and subsequently used in the sequencing reactions conducted using the BigDye Terminator v3.1 Cycle Sequencing Kit (4337455, Applied Biosystems, Thermo Fisher Scientific, USA). The resultant sequencing reactions were then purified and precipitated using the Ethanol/EDTA/Sodium Acetate precipitation method. Afterwards, capillary sequencing was carried out by Genetic Analyzer 3500 (Applied Biosystems, Thermo Fisher Scientific, USA). The sequences produced were then analyzed using Sequencing Analysis Software 6 (Applied Biosystems, Thermo Fisher Scientific, USA) and aligned with their respective published sequences of the *GJB2* (NM_004004.5) or the *TMEM59* (NM_001305066.1) genes using Basic Local Alignment Search Tool (BLAST) (https://blast.ncbi.nlm.nih.gov/Blast.cgi).

2.4. Mutational screening

A total of 107 HL patients and 50 healthy controls from the UAE were screened for the identified candidate variants. To screen for the *GJB2* variant (NM_004004.5: c.506G > A), Sanger sequencing was performed using the above-mentioned protocol. Whereas PCR-restriction fragment length polymorphism (RFLP) was used to screen for the *TMEM59* variant (NM_001305066.1: c.432_434del), as this deletion creates an SfaN1 restriction site. To carry out PCR-RFLP, PCR products were generated using primers gDNA_TM59_3F and gDNA_TM59_3R (Table 1). The produced amplicons were then digested by SfaN1 (R0172S, New England Biolabs, USA) according to the manufacturer's instructions and separated by 2% agarose gels to infer their respective genotypes.

2.5. Expression of the Tmem59 gene in mouse tissues

Expression of *Tmem59* was investigated in various mouse tissues including organ of Corti, brain, eyes, inner ear, lungs, heart, intestines, epididymal white adipose tissue, liver and kidneys using P1- P3 Swiss Jim Lambert (SJL) pups. Dissected tissues were immersed in 1% phosphate-buffered saline (10010023, ThermoFisher, Life Technologies) and immediately frozen in liquid nitrogen. Next, total RNA was extracted from these tissues using the RNeasy Mini Kit (74104, Qiagen, Germany) according to manufacturer's protocol. Afterwards, the SuperScript IV First-Strand Synthesis System (18091, Invitrogen, USA) was used to convert the extracted RNA into cDNA. The cDNA produced was then amplified by conventional PCR and quantitative PCR (qPCR) using primers cDNA_Mouse_1F and cDNA_Mouse_4R (Table 1) which span exons 1 to 4 in the murine *Tmem59* gene. Mouse Actb F and R primers (Table 1) were used to amplify the housekeeping gene *Actin beta* (*Actb)*. GoTaq qPCR Master Mix (A6001, Promega, USA) was used to carry out qPCR on the CFX96 Touch Real-Time PCR Detection System (1855195, BioRad, USA). All qPCR reactions were performed in triplicates and relative gene expression levels were determined by the delta Ct method. Experiments performed on SJL pups were approved by the University of Sharjah Research Ethics Committee and performed in accordance with the relevant guidelines and regulations established by the University of Sharjah Animal Care and Use Committee.

2.6. Minigene constructs

To validate the predicted impact of the *TMEM59* variant (NM_001305066.1: c.432_434del) on splicing; wildtype and corresponding mutant DNA fragments were cloned into a modified version of the p(13,17)-cytomegalovirus (CMV) vector which was kindly provided by Dr. Baklouti F (Ben Rebeh et al., 2010). In short, genomic DNA from individual IV-1 (Fig. 1) and a healthy control were amplified using primers TM59 _3F_BsteII and TM59_3R_NheI (Table 1). These PCR products were then each cloned into the p (13,17)-CMV vector via NheI (EN-146S, Jena Bioscience, Germany) and BstEII (R0162S, New England Biolabs, USA) restriction endonucleases generating the mutant pRc-CMV-DF and wildtype pRc-CMV-ctrl constructs respectively. Finally, these constructs were confirmed by Sanger sequencing using primer Ex13 (Table 1) by following the previously mentioned protocol.

2.7. Cell culture, transient transfection and cDNA synthesis

MG63 human osteosarcoma cells (CRL1427, ATCC, USA) were cultured in Dulbecco's Modified Eagle's Medium (D6429, Sigma-Aldrich, USA) supplemented with 10% fetal bovine serum (F9665, Sigma-Aldrich, USA) and 1% Penicillin-Streptomycin (P4333, Sigma-Aldrich, USA) in a 37 °C humidified atmosphere containing 5% CO_2. Cells were transiently transfected with 2500 ng of pRc-CMV-ctrl, pRc-CMV-DF or the empty p(13,17)-CMV vector using Lipofectamine 3000 reagent (L3000001, Invitrogen, USA) and incubated for 2 days according to manufacturer's protocol. Next, total RNA was extracted from transfected cells using the RNeasy Mini Kit (74104, Qiagen, Germany). Afterwards, the TruScript First Strand cDNA Synthesis Kit (54420, Norgen, Canada) was used to convert the extracted RNA into cDNA. The cDNA produced was then amplified using primers T7 and Sp6 (Table 1).

3. Results

3.1. Identification of candidate variants

A large consanguineous UAE family with bilateral severe to profound hearing loss was investigated in this study. Analysis of the family pedigree suggested a recessive mode of inheritance (Fig. 1 and Fig. 3 A). To identify candidate variants in this family, Sanger sequencing of the *GJB2* gene was performed for all available family members revealing the full segregation of the p.Cys169Tyr mutation. Next, to rule out the implication of any other variants WES was performed for individuals III-3, IV-1, IV-2, IV-4, and IV-5 (Fig. 1). Approximately 81,156,188 reads were generated for each individual with a read length of 151 bp. The panel coverage was more than 99% and the panel average depth was 134.786. Additionally, more than 95% of generated bases had a value of Q30.

WES generated a total of 628,908 variants collectively, among which 32,759 were non-synonymous, 864 were frameshift and 357 were stop-gained variants. All generated variants were filtered as follows: (1) only variants shared among all analyzed individuals were kept, (2) given the family's consanguinity and recessive inheritance pattern, homozygous variants identified within runs of homozygosity (ROH) equal to or greater than 3 Mb that segregated with the disease were kept (Supplementary Table S1), (3) variants described in dbSNP (https://www.ncbi.nlm.nih.gov/snp/), gnomAD (https://gnomad.broadinstitute.org/), or Ensembl (https://www.ensembl.org/index.html) with frequencies higher than 0.01% were excluded, and (4) variants found in our internal database that are common in the UAE population were also excluded. Among the 8 remaining homozygous variants (Table 2), an in-frame deletion and 3 missense variants were identified while the rest were all intronic. The missense variant NM_004519.4:c.1994C > T was predicted as "polymorphism" by MutationTaster, while the missense variant NM_173344.3:c.995A > G was predicted as "disease causing". However, these two variants were predicted as both "benign" and "tolerated" by PolyPhen and SIFT respectively and were therefore excluded. Consequently, only NM_004004.5: c.506G > A and NM_001305066.1: c.432_434del remained as candidate variants. The predicted impact of both can-

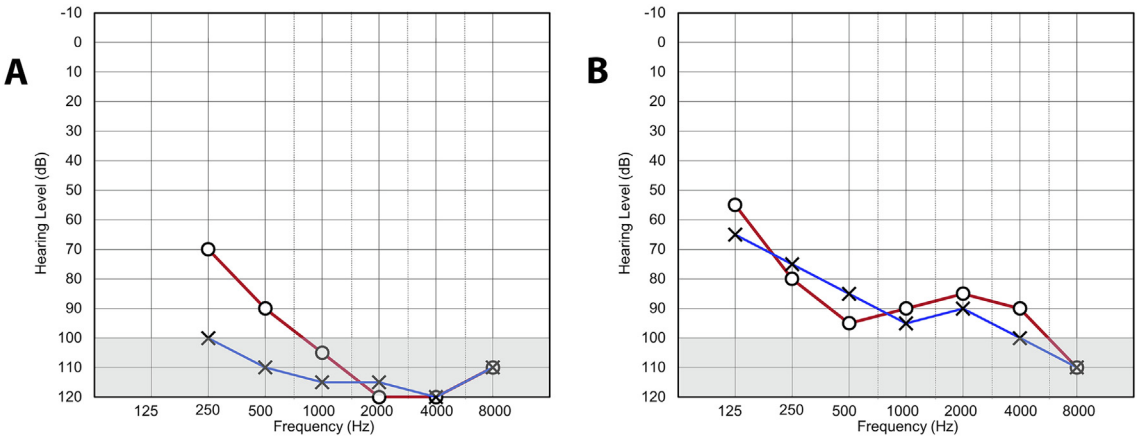

Fig. 3. Audiograms. (A) Audiogram of the proband. (B) Audiogram of an unrelated Emirati deaf individual homozygous for the *GJB2* p.Cys169Tyr mutation. Red lines indicate the right ear; blue lines indicate the left ear.

Table 2
Remaining variants after filtration of WES results.

Gene	Accession number	DNA change	Protein change	RS-ID	Type	Classification[1]	gnomAD allele frequencies[2]
Transmembrane Protein 59 (*TMEM59*)	NM_001305066.1	c.432_434delGCA	p. Trp144_His145delinsCys	rs375264930	Inframe deletion	Uncertain significance	0.001063
HERV-H LTR-Associating 1 (*HHLA1*)	NM_001145095.1	c.677-7C > T	NA	rs116232399	Intronic	Likely benign	0.001425
Potassium Voltage-Gated Channel Subfamily Q Member 3 (*KCNQ3*)	NM_004519.4	c.1994C > T	p.Ser665Leu	rs147173555	Missense	Benign	0.0003459
ST3 Beta-Galactoside Alpha-2,3-Sialyltransferase 1 (*ST3GAL1*)	NM_173344.3	c.995A > G	p.Asn332Ser	rs149294559	Missense	Uncertain significance	0.0009467
Gap Junction Protein Beta 2 (*GJB2*)	NM_004004.6	c.506G > A	p.Cys169Tyr	rs774518779	Missense	Uncertain significance	0.000007966
Estrogen-Related Receptor Alpha Pseudogene 2 (*ESRRAP2*)	NC_000013.10	n.533A > C	NA	rs368915924	Intronic	Uncertain significance	0.006665
Spermatogenesis Associated 13 (*SPATA13*)	NM_001166271.3	c.2667 + 66 T > C	NA	rs908890896	Intronic	Uncertain significance	0.00003194
C1q and TNF related 9 (*C1QTNF9*)	NM_178540.5	c.166 + 19C > T	NA	rs372292002	Intronic	Likely Benign	0.001414

[1] Classifications found at the beginning of the study. Recently, the c.423_434del variant has been re-classified as likely benign. All classifications are based on VarSome.
[2] Allele frequencies are based on gnomAD v2.1.1.

Table 3
Predicted impact of candidate variants by bioinformatic tools.

	c.506G > A	c.432_434del
MutationTaster	Disease causing	NA*
VarSome	Likely pathogenic	Uncertain significance *
VEP	Impact = moderate	NA
PolyPhen	Probably damaging	NA
PROVEAN	Deleterious	NA*
SIFT	Damaging	NA

NA: Not applicable.
* Classifications found at the beginning of the study. Recently, the c.423_434del variant has been re-classified as polymorphism, likely benign and neutral, by MutationTaster, VarSome and PROVEAN respectively.

didate variants was determined by several bioinformatics tools (Table 3).

To confirm the above findings, Sanger sequencing of the third exon of the *TMEM59* gene was carried out for the proband and individuals III-3, IV-1, IV-2, IV-4, and IV-5. Our results showed the same segregation pattern obtained for p.Cys169Tyr; where both III-3 and IV-4 were heterozygous for the *TMEM59* variant (Fig. 4 B and E), while the proband and the remaining affected siblings were homozygous (Fig. 4 A and D). None of the members of this HL family were homozygous for the wildtype genotype (Fig. 4 C and F). These findings indicate that both variants segregate with HL in this family.

3.2. Cochlear expression of murine Tmem59

Conventional and quantitative reverse transcription PCR (RT-qPCR) performed using RNA extracted from SJL mice showed that the *Tmem59* gene was expressed in the organ of Corti and most tested tissues except adipose tissue (Fig. 5 A and B). Furthermore, reverse transcription PCR (RT-PCR) of the housekeeping gene *Actb* showed that it was expressed in all tested tissues (Fig. 5 C).

3.3. Impact of the TMEM59 variant c.432_434del on splicing

The *TMEM59* variant (NM_001305066.1: c.432_434del) was predicted to cause the loss of a branch point in intron 3. Therefore, to validate the predicted impact of this variant on splicing; wild-type and corresponding mutant DNA fragments of the shortest isoform (ENST00000371337.3) were cloned into the p(13,17)-CMV vector. Sanger sequencing confirmed the sequences of mutant pRc-CMV-DF and wildtype pRc-CMV-ctrl constructs (Fig. 6). Moreover, RT-PCR performed using RNA extracted from MG63 cells transfected with pRc-CMV-DF showed no significant difference when compared to those transfected with pRc-CMV-ctrl.

3.4. Screening the UAE population for candidate variants

Screening the UAE population for the *GJB2* variant by Sanger sequencing revealed that it was absent in 103 unrelated deaf indi-

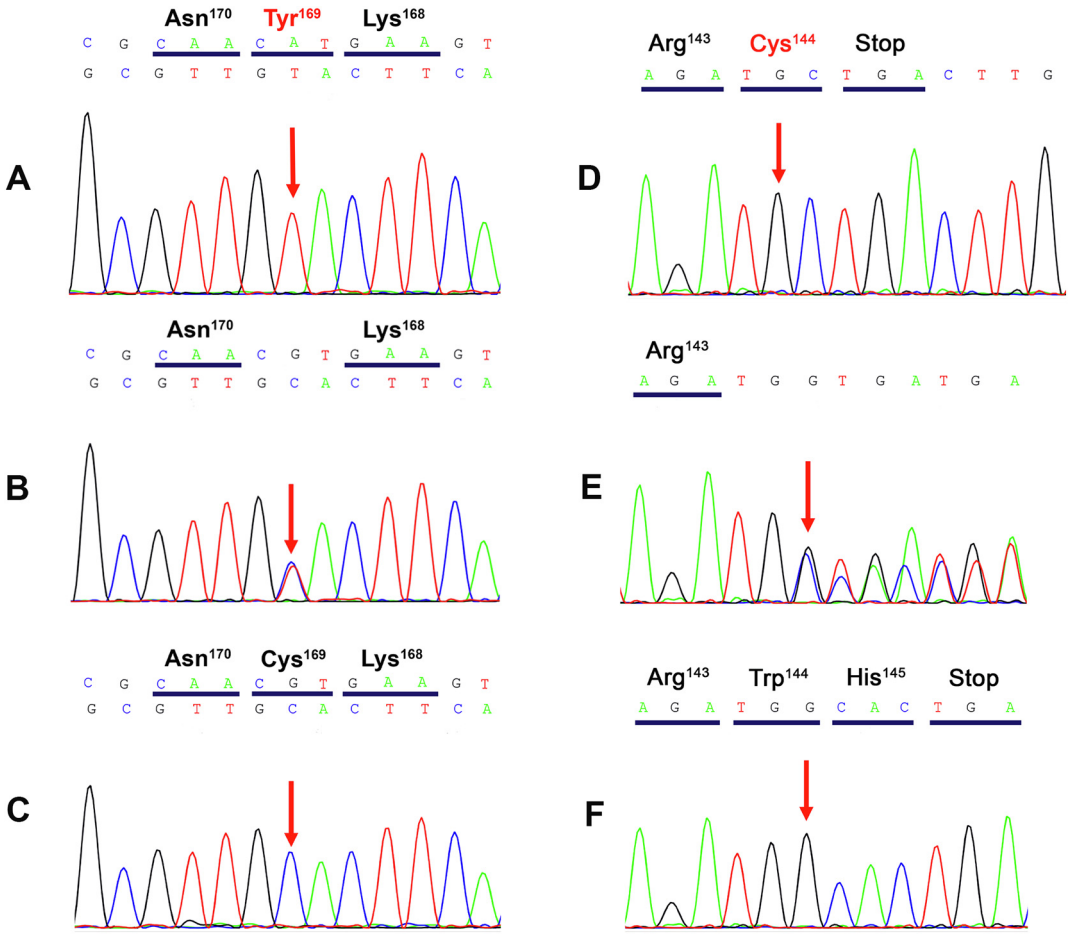

Fig. 4. Electropherograms. (A) Electropherogram of a homozygous mutant individual with the *GJB2* mutation c.506G > A. (B) Electropherogram of a heterozygous individual with the *GJB2* mutation c.506G > A. (C) Electropherogram of a homozygous wild-type individual. (D) Electropherogram of a homozygous mutant individual with the *TMEM59* variant c.432_434del. (E) Electropherogram of a heterozygous individual with the *TMEM59* variant c.432_434del. (F) Electropherogram of a homozygous wild-type individual.

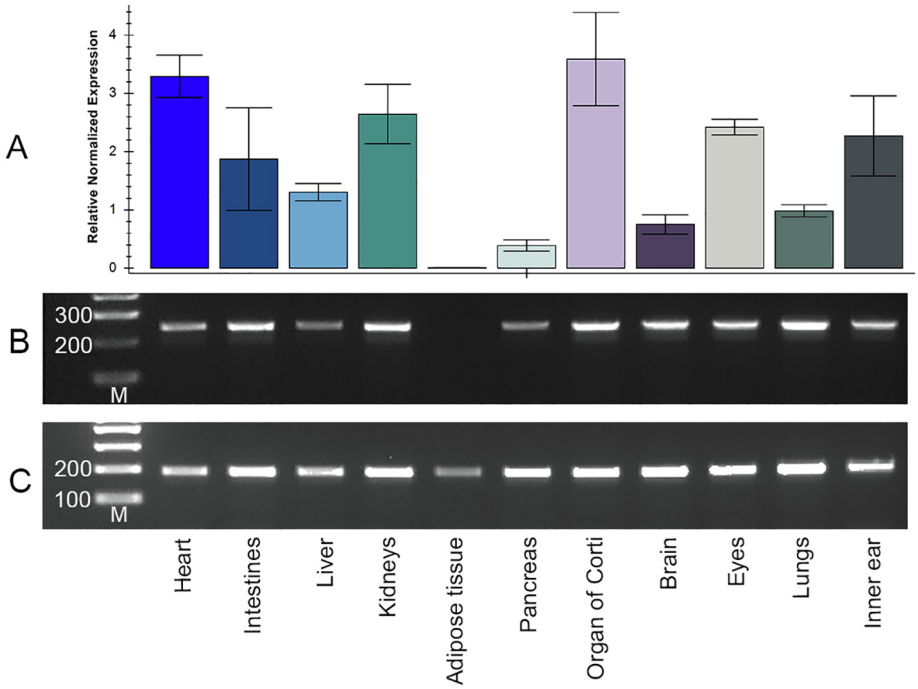

Fig. 5. RT-PCR analysis of *Tmem59* expression in mouse tissues. (A) Relative *Tmem59* expression in mouse tissues determined by RT-qPCR. (B) RT-PCR of the *Tmem59* gene in mouse tissues. (C) RT-PCR of the mouse housekeeping gene *ActB* in mouse tissues. M: 100 bp DNA ladder (Bioline, BIO-33056).

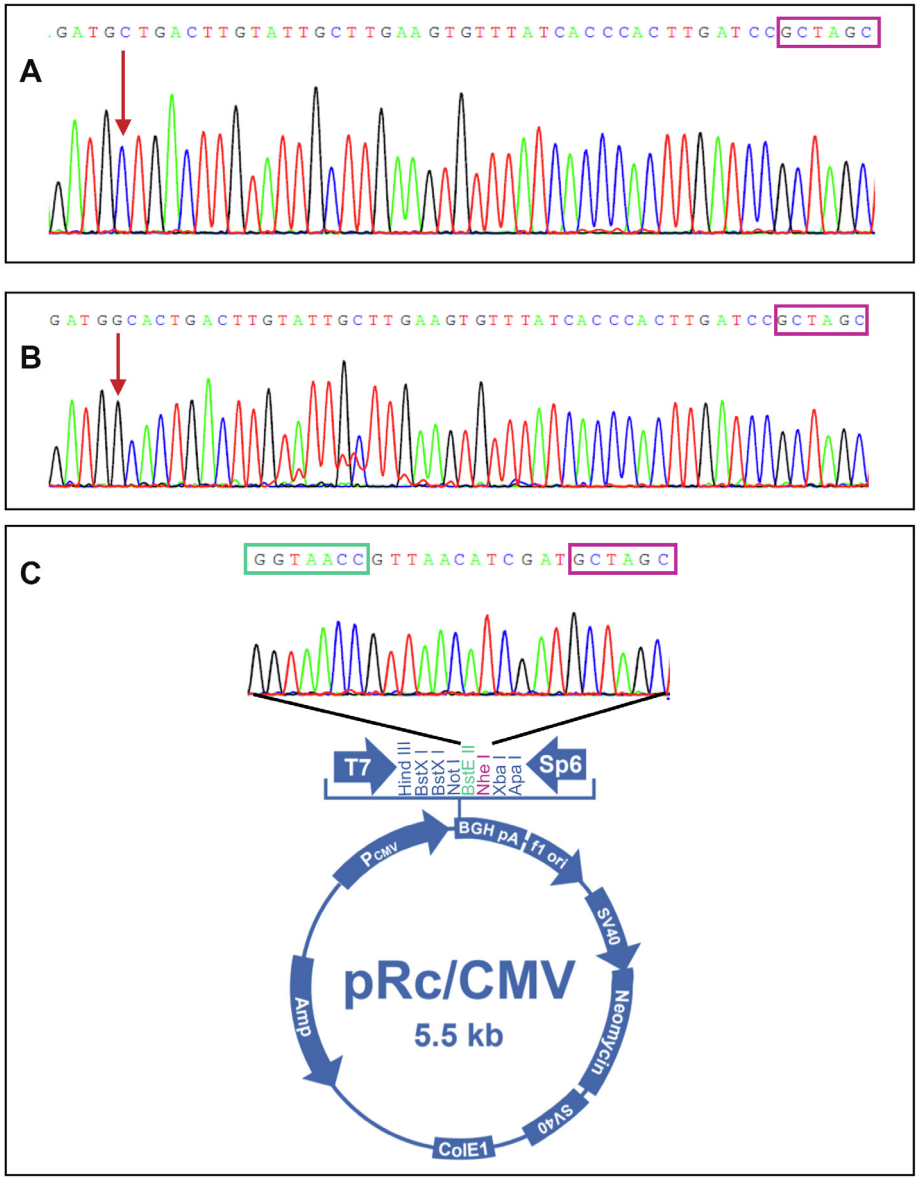

Fig. 6. Minigene constructions. (A) Electropherogram of pRC-CMV-DF. (B) Electropherogram of pRC-CMV-ctrl (C) Electropherogram of empty p(13,17)-CMV. Pink rectangle indicates the NheI restriction site. Green rectangle indicates the BstEII restriction site. Red arrow marks the position of the TMEM59 variant c.432_434del.

viduals and 50 healthy controls. Whereas screening the UAE population for the *TMEM59* variant by PCR-RFLP showed that it was present only in the heterozygous state in 3.7% (4/107) of the tested deaf individuals and 12% (6/50) of the control individuals, while it was absent in the rest.

4. Discussion

HL is the most common sensory defect with diverse and complex heterogeneity. Various molecular diagnostic techniques such as RFLP, Sanger sequencing and microarray have been widely utilized in detecting several HL mutations (Gibriel et al., 2019, Chakchouk et al., 2015). However, addressing such complexity necessitates the use of sophisticated NGS platforms for identification of causative HL mutations rapidly and efficiently (Souissi et al., 2021; Ben Ayed et al., 2021). In this study, we investigated a consanguineous Emirati family affected with NSHL. To identify the causative mutation in this family, Sanger sequencing of the *GJB2* gene, the most common ARNSHL gene in the UAE population (Tlili et al., 2017) was performed using the family's genomic DNA. This revealed the homozygous missense variant NM_004004.5: c.506G > A (p.Cys169Tyr). Given that this variant did not show full segregation with the HL phenotype in previous studies (Zonta et al., 2015; Birkenhager et al., 2014), WES was performed for the proband and available family members to rule out the implication of any other variants. Analysis of WES results followed by confirmation via Sanger sequencing allowed the identification of the homozygous *TMEM59* coding variant NM_001305066.1: c.432_434del (p.Trp144_His145delinsCys) as a second candidate variant in this HL family.

The *GJB2* gene encodes Cx26 which forms hemichannels that facilitate intercellular communication between neighboring cells. In the cochlea, Cx26 is expressed in the non-sensory cells (Liu and Zhao, 2008; Zhao and Yu, 2006) and has been implicated in many auditory processes the most popular being potassium homeostasis (Wingard and Zhao, 2015). However, although potassium recycling is an important aspect of the hearing process, recent studies have demonstrated that it is not a major deafness mecha-

Table 4
Published studies reporting the *GJB2* mutation p.Cys169Tyr.

Reference	Number of audiologically assessed patients with p.Cys169Tyr alleles	Ethnicity	HL severity	Segregation
Birkenhager et al., 2014	2	Middle eastern	Profound	Partial
Alkowari et al. 2012 and Zonta et al. 2015	6	Qatari	Moderate to severe	Partial
Tlili et al. 2017 and this study	2	Emirati	Severe to profound	Full

nism as Cx26 deficiency can have different underlying deafness mechanisms rather than a unique deafness mechanism as assumed by the K^+ recycling hypothesis (Zhu et al., 2013; Zhu et al., 2015a; Liang et al., 2012; Zhu et al., 2015b). These conflicting issues often hinder our understanding of the exact role played by *GJB2*, the most prominent deafness gene.

The *GJB2* variant c.506G > A (p.Cys169Tyr) initially classified as a polymorphism (Azaiez et al., 2004; Khalifa Alkowari et al., 2012); was first reported as pathogenic when identified in the homozygous state in an extended consanguineous middle-eastern family with congenital HL (Birkenhager et al., 2014). Shortly after, this mutation was reported in other consanguineous families with congenital HL of varying severity (Zonta et al., 2015). Surprisingly, despite the consanguinity and the recessive inheritance of the investigated families, both studies showed partial segregation of this variant with the HL phenotype. In 2017, Tlili et al. identified this mutation in the homozygous state in three unrelated UAE deaf individuals, one of which was the proband of the HL family presented here (Tlili et al., 2017). In contrast to the previous p. Cys169Tyr studies, we demonstrate full segregation of this variant with the HL phenotype. Comparing the phenotypes of the proband in this study (Fig. 3 A), another unrelated Emirati homozygous individual (Fig. 3 b) and all reported studies we found that severe to profound HL is the most common which is consistent with most *GJB2* related deafness (Kenneson et al., 2002). However, we were unable to establish a clear genotype-phenotype correlation as individuals heterozygous for p.Cys169Tyr have showed both moderate and severe HL in previous studies (Table 4). This discrepancy in HL severity among patients with p.Cys169Tyr alleles may be linked to other unknown genetic or environmental factors. Furthermore, to better understand the distribution of p.Cys169Tyr in the UAE we screened 103 unrelated HL patients and 50 deafness free controls. The absence of this mutation in this cohort and its low frequency in gnomAD (0.000007966) indicates that it is relatively uncommon in many populations.

The c.506G > A (p.Cys169Tyr) mutation destroys the third disulfide bridge between cysteine residues 64 and 169 in the Cx26 protein. The absence of this bond is expected to alter the three-dimensional structure of this protein, ultimately inhibiting low-molecular substance exchange between connexons of neighboring cells (Birkenhager et al., 2014). In fact, immunofluorescence of HeLa cells expressing this mutation showed that the mutated protein is properly trafficked to the plasma membrane but is unable to form gap-junction plaques (Zonta et al., 2015). Collectively, the above evidence reinforces the pathogenicity of the p.Cys169Tyr variant.

The second candidate variant identified in the present study was within the *TMEM59* gene. The TMEM59 protein belongs to a family of transmembrane proteins with mostly unknown functions (Marx et al., 2019). So far, the TMEM132E protein is the only member of this family to be linked to hereditary hearing loss and has been suggested to play a role in neuronal function and mammalian cochlear development and hearing (Liaqat et al., 2019; Li et al., 2015). Similarly, the TMEM59 protein is also thought to play a role in the neural system (Ullrich et al., 2010) and to be a positive regulator of Wnt signaling (Gerlach et al., 2018) which is a crucial signaling pathway in the inner ear. Given the segregation of the identified *TMEM59* variant (NM_001305066.1: c.432_434del) with HL in the present study, we tested different mouse tissues for the expression of this gene. Our results were similar to the *TMEM132E* study, as *Tmem59* was expressed in the majority of tested tissues including the organ of Corti. Furthermore, we examined the expression of the *Tmem59* gene using the gene Expression Analysis Resource (gEAR) portal which displays data from mouse organ of Corti at postnatal day P0 – P7 (https://umgear.org/) and found that it was detected in both supporting cells and hair cells, the latter of which showed slightly higher expression. The above preliminary findings suggest a possible link between *TMEM59* and hearing. Nevertheless, in vitro and in silico evidence as well as investigating the localization of the *TMEM59* gene within the cochlea is vital to confirm its involvement in the hearing mechanism.

The *TMEM59* variant NM_001305066.1: c.432_434del identified in this study, is located in the coding region of the shortest *TMEM59* isoform only (ENST00000371337.3), where it is located 173 bases away from the nearest splice site and is predicted by the Human Splicing Finder to cause the loss of a branch point in intron 3. Due to the possible involvement of *TMEM59* in hearing we decided to further study the c.432_434del variant. To test the impact of this variant on splicing, MG63 cells were transfected with pRc-CMV-DF, pRc-CMV-ctrl or p(13,17)-CMV. RT-PCR results showed that there is no difference in the splicing pattern obtained for pRc-CMV-DF and pRc-CMV-ctrl, suggesting that this *TMEM59* deletion has no impact on splicing. Screening the UAE population for the c.432_434del variant showed that it was present in the heterozygous state in 6.4% (10/157) of the tested individuals while none of the rest were homozygous for this variant. Moreover, in gnomAD c.432_434del has a frequency of 0.001063 which is much higher than the *GJB2* variant. However, although further screening is required to classify c.432_434del has as a polymorphism, the lack of evidence linking this variant to the HL phenotype as well as the pathogenicity of the *GJB2* variant indicates that c.506G > A (p.Cys169Tyr) is the causative mutation in this HL family.

Lastly, it is important to note that while segregation with disease phenotype is an indispensable tool in genetic diagnosis, our findings reinforce that it should not be the sole approach used. In this study, the analysis of all available family members revealed several variants that segregated with HL which is expected given the size and consanguinity of the family. The use of WES played an instrumental role in narrowing down these variants to the two candidate variants mentioned above. Therefore, we recommend performing WES prior to reaching a final diagnosis.

5. Conclusion

In this study, WES in combination with segregation, in silico, splicing and expression analyses confirmed the causality of the *GJB2* missense mutation p.Cys169Tyr in a consanguineous Emirati family with severe to profound hearing loss. The findings and approaches presented here are important in the molecular diagnosis of hereditary hearing loss in highly consanguineous populations such as the UAE.

Declaration of Competing Interest

The authors declare that they have no known competing financial interests or personal relationships that could have appeared to influence the work reported in this paper.

Acknowledgements

We greatly appreciate the family included in this study for their patience and full cooperation. This work was supported by the University of Sharjah and Sheikh Hamdan Bin Rashid Al-Maktoum Award for Medical Sciences.

Appendix A. Supplementary material

Supplementary data to this article can be found online at https://doi.org/10.1016/j.sjbs.2021.04.036.

References

Azaiez, H., Chamberlin, G.P., Fischer, S.M., Welp, C.L., Prasad, S.D., Taggart, R.T., del Castillo, I., Van Camp, G., Smith, R.J., 2004. GJB2: the spectrum of deafness-causing allele variants and their phenotype. Hum. Mutat. 24, 305–311.

Ben Ayed, I., Ouarda, W., Frikha, F., Kammoun, F., Souissi, A., Ben Said, M., Bouzid, A., Elloumi, I., Hamdani, T.M., Gharbi, N., Baklouti, N., Guirat, M., Mejdoub, F., Kharrat, N., Boujelbene, I., Abdelhedi, F., Belguith, N., Keskes, L., Gibriel, A.A., Kamoun, H., Triki, C., Alimi, A.M., Masmoudi, S., 2021. SRD5A3-CDG: 3D structure modeling, clinical spectrum, and computer-based dysmorphic facial recognition. Am. J. Med. Genet. A. 185, 1081–1090.

Ben Rebeh, I., Moriniere, M., Ayadi, L., Benzina, Z., Charfedine, I., Feki, J., Ayadi, H., Ghorbel, A., Baklouti, F., Masmoudi, S., 2010. Reinforcement of a minor alternative splicing event in MYO7A due to a missense mutation results in a mild form of retinopathy and deafness. Mol. Vis. 16, 1898–1906.

Birkenhager, R., Prera, N., Aschendorff, A., Laszig, R., Arndt, S., 2014. A novel homozygous mutation in the EC1/EC2 interaction domain of the gap junction complex connexon 26 leads to profound hearing impairment. Biomed. Res. Int. 2014, 307976.

Bouzid, A., Smeti, I., Chakroun, A., Loukil, S., Gibriel, A.A., Grati, M., Ghorbel, A., Masmoudi, S., 2018a. CDH23 Methylation Status and Presbycusis Risk in Elderly Women. Front. Aging Neurosci. 10, 241.

Bouzid, A., Smeti, I., Dhouib, L., Roche, M., Achour, I., Khalfallah, A., Gibriel, A.A., Charfeddine, I., Ayadi, H., Lachuer, J., Ghorbel, A., Petit, C., Masmoudi, S., 2018b. Down-expression of P2RX2, KCNQ5, ERBB3 and SOCS3 through DNA hypermethylation in elderly women with presbycusis. Biomarkers 23, 347–356.

Chakchouk, I., Ben Said, M., Jbeli, F., Benmarzoug, R., Loukil, S., Smeti, I., Chakroun, A., Gibriel, A.A., Ghorbel, A., Hadjkacem, H., Masmoudi, S., 2015. NADf chip, a two-color microarray for simultaneous screening of multigene mutations associated with hearing impairment in North African Mediterranean countries. J. Mol. Diagn. 17, 155–161.

Chan, D.K., Chang, K.W., 2014. GJB2-associated hearing loss: systematic review of worldwide prevalence, genotype, and auditory phenotype. Laryngoscope 124, E34–53.

Gerlach, J.P., Jordens, I., Tauriello, D.V.F., van 't Land-Kuper, I., Bugter, J.M., Noordstra, I., van der Kooij, J., Low, T.Y., Pimentel-Muinos, F.X., Xanthakis, D., Fenderico, N., Rabouille, C., Heck, A.J.R., Egan, D.A., Maurice, M.M., 2018. TMEM59 potentiates Wnt signaling by promoting signalosome formation. Proc. Natl. Acad. Sci. U. S. A. 115, E3996-E4005.

Gibriel, A.A., Abou-Elew, M.H., Masmoudi, S., 2019. Analysis of p.Gly12Valfs*2, p.Trp24* and p.Trp77Arg mutations in GJB2 and p.Arg81Gln variant in LRTOMT among non syndromic hearing loss Egyptian patients: implications for genetic diagnosis. Mol. Biol. Rep. 46, 2139–2145.

Kelsell, D.P., Dunlop, J., Stevens, H.P., Lench, N.J., Liang, J.N., Parry, G., Mueller, R.F., Leigh, I.M., 1997. Connexin 26 mutations in hereditary non-syndromic sensorineural deafness. Nature 387, 80–83.

Kenneson, A., Van Naarden Braun, K., Boyle, C., 2002. GJB2 (connexin 26) variants and nonsyndromic sensorineural hearing loss: a HuGE review. Genet. Med. 4, 258–274.

Khalifa Alkowari, M., Girotto, G., Abdulhadi, K., Dipresa, S., Siam, R., Najjar, N., Badii, R., Gasparini, P., 2012. GJB2 and GJB6 genes and the A1555G mitochondrial mutation are only minor causes of nonsyndromic hearing loss in the Qatari population. Int. J. Audiol. 51, 181–185.

Kumar, P., Henikoff, S., Ng, P.C., 2009. Predicting the effects of coding non-synonymous variants on protein function using the SIFT algorithm. Nat. Protoc. 4, 1073–1081.

Li, H., Durbin, R., 2010. Fast and accurate long-read alignment with Burrows-Wheeler transform. Bioinformatics 26, 589–595.

Li, H., Handsaker, B., Wysoker, A., Fennell, T., Ruan, J., Homer, N., Marth, G., Abecasis, G., Durbin, R., 1000 Genome Project Data Processing Subgroup, 2009. The Sequence Alignment/Map format and SAMtools. Bioinformatics 25, 2078-2079.

Li, J., Zhao, X., Xin, Q., Shan, S., Jiang, B., Jin, Y., Yuan, H., Dai, P., Xiao, R., Zhang, Q., Xiao, J., Shao, C., Gong, Y., Liu, Q., 2015. Whole-exome sequencing identifies a variant in TMEM132E causing autosomal-recessive nonsyndromic hearing loss DFNB99. Hum. Mutat. 36, 98–105.

Liang, C., Zhu, Y., Zong, L., Lu, G.J., Zhao, H.B., 2012. Cell degeneration is not a primary causer for Connexin26 (GJB2) deficiency associated hearing loss. Neurosci. Lett. 528, 36–41.

Liaqat, K., Hussain, S., Bilal, M., Nasir, A., Acharya, A., Ali, R.H., Nawaz, S., Umair, M., Schrauwen, I., Ahmad, W., Leal, S.M., 2019. Further evidence of involvement of TMEM132E in autosomal recessive nonsyndromic hearing impairment. J. Hum Genet.

Liu, Y.P., Zhao, H.B., 2008. Cellular characterization of Connexin26 and Connnexin30 expression in the cochlear lateral wall. Cell Tissue Res. 333, 395–403.

Marazita, M.L., Ploughman, L.M., Rawlings, B., Remington, E., Arnos, K.S., Nance, W. E., 1993. Genetic epidemiological studies of early-onset deafness in the U.S. school-age population. Am. J. Med. Genet. 46, 486–491.

Marx, S., Dal Maso, T., Chen, J.W., Bury, M., Wouters, J., Michiels, C., Le Calve, B., 2019. Transmembrane (TMEM) protein family members: Poorly characterized even if essential for the metastatic process. Semin. Cancer Biol.

McKenna, A., Hanna, M., Banks, E., Sivachenko, A., Cibulskis, K., Kernytsky, A., Garimella, K., Altshuler, D., Gabriel, S., Daly, M., DePristo, M.A., 2010. The Genome Analysis Toolkit: a MapReduce framework for analyzing next-generation DNA sequencing data. Genome Res. 20, 1297–1303.

Morton, C.C., Nance, W.E., 2006. Newborn hearing screening–a silent revolution. N. Engl. J. Med. 354, 2151–2164.

Sohl, G., Willecke, K., 2004. Gap junctions and the connexin protein family. Cardiovasc. Res. 62, 228–232.

Souissi, A., Ben Said, M., Ben Ayed, I., Elloumi, I., Bouzid, A., Mosrati, M.A., Hasnaoui, M., Belcadhi, M., Idriss, N., Kamoun, H., Gharbi, N., Gibriel, A.A., Tlili, A., Masmoudi, S., 2021. Novel pathogenic mutations and further evidence for clinical relevance of genes and variants causing hearing impairment in Tunisian population. J. Adv. Res.

Tlili, A., Al Mutery, A., Kamal Eddine Ahmad Mohamed, W., Mahfood, M., Hadj Kacem, H., 2017. Prevalence of GJB2 Mutations in Affected Individuals from United Arab Emirates with Autosomal Recessive Nonsyndromic Hearing Loss. Genet. Test. Mol. Biomarkers 21, 686–691.

Ullrich, S., Munch, A., Neumann, S., Kremmer, E., Tatzelt, J., Lichtenthaler, S.F., 2010. The novel membrane protein TMEM59 modulates complex glycosylation, cell surface expression, and secretion of the amyloid precursor protein. J. Biol. Chem. 285, 20664–20674.

Vona, B., Nanda, I., Hofrichter, M.A., Shehata-Dieler, W., Haaf, T., 2015. Non-syndromic hearing loss gene identification: A brief history and glimpse into the future. Mol. Cell. Probes 29, 260–270.

Wingard, J.C., Zhao, H.B., 2015. Cellular and Deafness Mechanisms Underlying Connexin Mutation-Induced Hearing Loss - A Common Hereditary Deafness. Front. Cell. Neurosci. 9, 202.

Zhao, H.B., Yu, N., 2006. Distinct and gradient distributions of connexin26 and connexin30 in the cochlear sensory epithelium of guinea pigs. J. Comp. Neurol. 499, 506–518.

Zhu, Y., Chen, J., Liang, C., Zong, L., Chen, J., Jones, R.O., Zhao, H.B., 2015a. Connexin26 (GJB2) deficiency reduces active cochlear amplification leading to late-onset hearing loss. Neuroscience 284, 719–729.

Zhu, Y., Liang, C., Chen, J., Zong, L., Chen, G.D., Zhao, H.B., 2013. Active cochlear amplification is dependent on supporting cell gap junctions. Nat. Commun. 4, 1786.

Zhu, Y., Zong, L., Mei, L., Zhao, H.B., 2015b. Connexin26 gap junction mediates miRNA intercellular genetic communication in the cochlea and is required for inner ear development. Sci. Rep. 5, 15647.

Zonta, F., Girotto, G., Buratto, D., Crispino, G., Morgan, A., Abdulhadi, K., Alkowari, M., Badii, R., Gasparini, P., Mammano, F., 2015. The p.Cys169Tyr variant of connexin 26 is not a polymorphism. Hum. Mol. Genet. 24, 2641–2648.